# Quantification of streamflow response to climate change and human activities within upstream mountainous areas of the Daqing River Basin, Northern China

Zengyi Li[1], Weifan Chen[2]* and Linna Wang[2]

[1]School of Water Conservancy, North China University of Water Resources and Electric Power, Zhengzhou, China, [2]State Key Laboratory of Simulation and Regulation of Water Cycle in River Basin, China Institute of Water-Resources and Hydropower Research, Beijing, China

The Daqinghe River Basin is located in the North China Plain. In recent years, however, climate warming, drying, and intense human activities have led to declining ecosystem functions and shrinking wetlands in the region. Understanding streamflow changes in the upstream mountainous areas of the Daqinghe River Basin in this changing environment and identifying the driving factors can provide a scientific basis for water resources management and optimization in these areas. This study focuses on the Beihedian River watershed, the Xidayang Reservoir watershed, and the Wangkuai Reservoir watershed in the upstream mountainous areas of the Daqinghe River. It is based on hydro-meteorological data collected between 1963 and 2019. The methods used in the study include the linear tendency estimation method, the non-parametric Mann-Kendall trend test, the elasticity coefficient method, and hydrological simulation methods. The results of this study suggest that the streamflow, precipitation, and potential evapotranspiration (PET) in the three watersheds showed an overall decreasing trend. The minimum precipitation decrease rate ranged from −1.09 to −0.55 mm/a, and the minimum streamflow decreasing rate at the Beihedian Hydrological Station was −1.32 mm/a, with a minimum range of 0−176.03 mm. Change-point analysis revealed that the streamflow in the Beihedian River and Xidayang Reservoir watersheds experienced a significant change point around 1999, with a significant level of $\alpha=0.05$. As for the Wangkuai Reservoir watershed, a significant change point was observed around 1980, which is likely attributable to land system reforms and protective forest projects. The attribution analysis which combined both climate change and human activities using the elasticity coefficient method and hydrological simulation methods indicated that climate change contributed an average of 32.93%, 34.50%, and 35.12% to the reduction in streamflow in the three watersheds, respectively. Human activities accounted for an average contribution of 67.07%, 65.50%, and 64.88%, respectively. Water conservancy projects, afforestation, and other human activities were identified as the primary factors contributing to streamflow decreases.

KEYWORDS

streamflow, land use change, climate change, human activities, hydrological simulation method

# 1 Introduction

On a global scale, climate change and human activities are affecting the water cycle in many watersheds (Chien et al., 2013; Liu et al., 2020). Climate change including global warming and other related issues profoundly affects hydrological processes such as precipitation and evaporation, which exhibit varying temporal and spatial distributions. It can also lead to an increased frequency of extreme weather events (Wu et al., 2021; Yang et al., 2019). In the past 40 years, significant human activities have had an undeniable impact on hydrological processes within the watershed (Lyu et al., 2024; Zhang et al., 2023). Human activities primarily influence hydrological cycling by altering the structure of underlying surfaces (Zhang and Yu, 2021). Therefore, human activities within the watershed are also one of the main causes of river evolution (Deng et al., 2024; Zheng et al., 2023). In this context, understanding the hydrological evolution under changing environments and quantifying the impact of various factors on streamflow is crucial for water resource management and sustainable development (Liu et al., 2020; Jiang et al., 2015; Liang et al., 2015; Zeng et al., 2020).

Baiyangdian Lake, situated within the Daqing River System in the Haihe River Basin, is of significant importance. The lake plays an irreplaceable role in maintaining the ecological balance of North China, regulating the climate in the Beijing-Tianjin-Hebei region, replenishing groundwater resources, alleviating floods and droughts, and preserving biodiversity and rare species (Moiwo et al., 2010; Song et al., 2018; Zerizghi et al., 2020). The upstream areas of the Daqing River Basin include eight rivers that flow into the lake, contributing an average annual streamflow volume of 2.23 billion m³ and an average streamflow depth of 71.5 mm (Liu et al., 2022). The upstream mountainous areas in the western part of the basin are the primary catchment areas, accounting for 85% of the total streamflow. However, the water resources situation in the Daqing River Basin has become increasingly challenging due to the combined effects of climate warming, drying in North China, and intense human activities since the 1960s (Cheng et al., 2017; Wang et al., 2021; Yang and Cao, 2021). This has led to a growing conflict between water resource availability and economic development (Song et al., 2018; Dai et al., 2011; Xu et al., 2013). Given that the upstream mountainous areas are crucial as primary water sources in the Daqing River Basin (Hu et al., 2012), understanding the main causes of streamflow decline in these regions is essential for the rational development and effective allocation of water resources within the basin. It also supports the implementation of scientifically informed water resource management practices.

Numerous studies have investigated the evolution and causes of streamflow changes in the Daqing River Basin. Lei et al. used a process-based terrestrial model (version 4 of the Community Land Model, CLM4) to quantify the spatiotemporal variation in streamflow across the region due to climate factors and changes in carbon dioxide concentration. Their results indicate a decreasing trend in streamflow related to climate since 1960, with a limited impact from the rise in atmospheric $CO_2$ concentration (Lei et al., 2014). Du et al. developed a monthly ABCD model for the Yongding River Basin and two subbasins, the Yanghe and Sanggan Rivers, to assess the relative contributions of climate change and human activities to streamflow reduction. They found a significant decline in annual streamflow since the 1980s, with human activities

being the predominant influencing factor, especially during the rainy season (Du et al., 2023). Li et al. employed the Statistical DownScaling Model (SDSM) to downscale predicted precipitation and temperature for the mountainous Yongding watershed under four SSP-RCP climate scenarios across four General Circulation Models (GCMs). The Bayesian Model Averaging (BMA) method was then used for multi-model integration to mitigate GCM uncertainty, and the multi-model ensemble data were adjusted using the Quantile Mapping (QM) method. Subsequently, the SWAT model was applied to simulate streamflow responses under future climate conditions (Li et al., 2023). Qiao et al. applied two methods, the watershed water-energy balance equation and the Geomorphology-Based Hydrological Model (GBHM), to study streamflow changes in a semiarid mountainous watershed. Their findings revealed a significant downward trend in streamflow and leaf area index (LAI) over the past 40 years, with different interdecadal quantitative results from the two methods. GBHM, in particular, struggled to accurately simulate reservoir scheduling and other processes (Qiao et al., 2023). Zhang et al. calculated multi-year averages of 17 environmental variables from 57 selected watersheds, including hydrological, meteorological, vegetation, land use, terrain, and soil data. They established a quantitative relationship between streamflow and watershed area for the first time and evaluated the correlation between environmental factors and the impact on streamflow scale (Zhang et al., 2019). Wang et al. used the Mann-Kendall test, double cumulative curve method, and streamflow sensitivity analysis to separate and quantify the relative effects of climate variability and land use changes on streamflow. Then they estimated the sensitivity of streamflow in North China from 1957 to 2000 to these factors (Wang et al., 2019). Huang et al. developed an extended Budyko framework incorporating Total Water Storage (TWS) from the Gravity Recovery and Climate Experiment (GRACE), and applied it to the Qinba Mountain area by four classic Budyko equations. Their results indicated that the extended Budyko framework more accurately represents the relationship between monthly water supply and demand compared to the original framework (Huang et al., 2021).

This study specifically targets three primary streamflow-producing areas located in the upstream mountainous regions of the Daqing River Basin. By comprehensively analyzing the trends in water cycle elements, the study employs both the elasticity coefficient method and the hydrological simulation method to determine the causes of water resource depletion within the basin. Additionally, it quantitatively examines the sensitivity of streamflow to variations in various driving factors and assesses the respective contribution rates of climate change and human activities to streamflow variation. The ultimate objective of this study is to provide scientific references for improving water resource management within the watershed and implementing effective measures for managing small watersheds.

# 2 Materials and methods

## 2.1 Study area

The study area is located in the upstream mountainous regions of the western Daqing River Basin and includes three hydrological
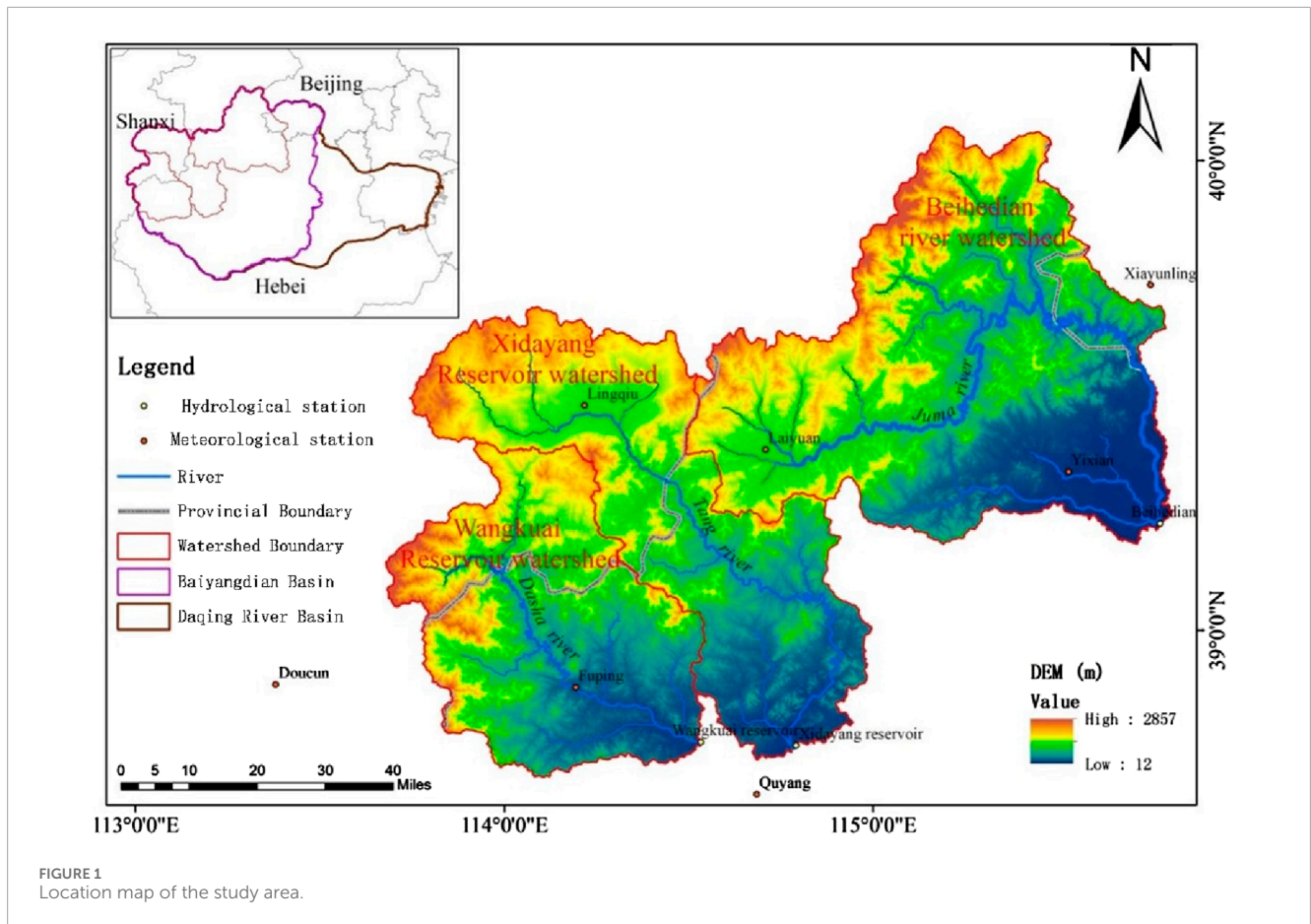
**FIGURE 1**
Location map of the study area.

stations: Beihedian Station, Xidayang Reservoir Station, and Wangkuai Reservoir Station (Figure 1). Geographically, it is located between 113°39′–115°48′E and 38°39′–40°03′N, covering a total area of 15,028 km². The terrain generally exhibits high elevation in the northwest and low elevation in the southeast, with an average altitude of 868.42 m and the highest point reaching 2,857 m (Figure 1). The study area experiences a temperate semiarid continental monsoon climate, characterized by four distinct seasons. Rain and heat often occur simultaneously. Spring is characterized by little rainfall and low humidity, while summer is hot and rainy. Autumn is typically clear with moderate temperatures, and winter is cold with little precipitation. The average annual precipitation in the study area is 533 mm, and the average annual PET is 817 mm. Precipitation is unevenly distributed throughout the year, with the majority of rainfall occurring from June to September. Additionally, there is significant interannual variability in rainfall, which can lead to both droughts and floods.

## 2.2 Data sources and Preprocessing

The data required for this study include meteorological and hydrological station observation data, Digital Elevation Model (DEM) data, land use type data, and Normalized Difference Vegetation Index (NDVI) data. Seven national meteorological

stations located in the upstream mountainous areas of the Daqing River Basin were carefully selected for this study. Daily observation data covering the period from 1963 to 2019 were obtained from the China Meteorological Data Service Centre (http://data.cma.cn/). The dataset includes various meteorological parameters such as average temperature, maximum and minimum temperature, precipitation, wind speed, sunshine duration, relative humidity, and vapor pressure. To address missing data, temporal and spatial interpolation methods were applied. Spatial interpolation was used when nearby stations with similar natural conditions to the stations with missing data were available, while temporal interpolation was performed by data from the same period in adjacent years when spatial interpolation was not possible. The PET was estimated by the Penman-Monteith equation recommended by the Food and Agriculture Organization (FAO). The basin-scale precipitation and PET data were obtained through the inverse distance weighting (IDW) interpolation method. Daily streamflow observation data from Wangkuai Reservoir, Xidayang Reservoir, and Beihedian hydrological stations, spanning 1963 to 2019, were sourced from the Hebei Hydrological Survey and Research Center and the Baoding Hydrological Survey and Research Center. The DEM data were acquired from the Geospatial Data Cloud (http://www.gscloud.cn/). The land use type data and NDVI data used in the study were obtained from the Resource and Environment Science and Data Center of the Chinese Academy of Sciences (https://www.resdc.cn/).

## 2.3 Methodology

### 2.3.1 Trend analysis

The trend patterns of hydrometeorological variables in the Daqing River Basin were analyzed using the linear propensity estimation and the non-parametric Mann-Kendall trend test methods.

#### 2.3.1.1 Linear propensity estimation method

The linear propensity estimation method was employed to establish a simple linear regression equation that reflects the changes in hydrometeorological variables over time. The formula is shown in Equation 1

$$y = ax + b \tag{1}$$

where $x$ is the sequential value of years; $y$ is the value of the hydrometeorological variable corresponding to the year $x$; $a$ is the regression coefficient, with positive and negative signs indicating an upward or downward trend, respectively; and $b$ is the regression constant.

#### 2.3.1.2 Mann-Kendall trend test method

The Mann-Kendall (MK) test method is a widely used approach for testing trends in hydro-meteorological variables, including temperature, precipitation, and streamflow. This method does not require samples to follow a specific distribution and can directly assess change in the variables. When performing a trend test on a given sequence $X\{x_i, i = 1, 2, \ldots, n\}$ with $n$ samples, the test statistic Z is calculated by the following formula 2:

$$Z = \begin{cases} \dfrac{S - 1}{\sqrt{\text{Var}(s)}} & S > 0 \\ 0 & S = 0 \\ \dfrac{S + 1}{\sqrt{\text{Var}(s)}} & S < 0 \end{cases} \tag{2}$$

where, $n$ is the length of the hydrometeorological variable sequence. $S$ is calculated by the following formula 3:

$$S = \sum_{i=1}^{n-1} \sum_{j=i+1}^{n} sgn\left(x_j - x_i\right) \quad (j = 2, 3, 4, \ldots, n) \tag{3}$$

where $x_i$ and $x_j$ are the hydrometeorological variable values for the $i$-th and $(i+1)$-th years, respectively. The function $sgn(\cdot)$ is calculated by the following formula 4:

$$sgn\left(x_j - x_i\right) = \begin{cases} 1, & x_j > x_i \\ 0, & x_j = x_i \\ -1, & x_j < x_i \end{cases} \tag{4}$$

When the sample size $n$ is sufficiently large, the variance $Var(s)$ of the test statistic $S$ is calculated by the following expression Equation 5:

$$Var(s) = \frac{n(n - 1)(2n + 5)}{18} \tag{5}$$

The Mann-Kendall method utilizes the test statistic $Z$ to assess the trend of the hydro-meteorological variable sequence. A positive

value of $Z$ $(Z > 0)$ indicates an upward trend while a negative value $(Z < 0)$ indicates a downward trend. The magnitude of $Z$ reflects the significance of the change in the sequence. When $|Z| > Z_{1-\frac{\alpha}{2}}$, the variable exhibits a significant upward or downward trend at the significance level α. The critical value required for the test, $\pm Z_{1-\frac{\alpha}{2}}$, can be obtained by referencing a table.

### 2.3.2 Abrupt change analysis

The Pettitt method is used for detecting abrupt change points by directly analyzing rank sequences. The change point $k$ is identified at time $t_0$ if the following condition is satisfied as represented by the following formula 6:

$$k_{t_0} = Max|S_k| \quad (k = 2, 3, \cdots, n) \tag{6}$$

Then $t_0$ is considered as an abrupt change point. Here, the rank sequence $S_k$ is the cumulative count of values at time $i$ that is greater or less than the values at time $j$, where $j = 1, 2, \ldots, i$.

The statistical significance level of an abrupt change point is determined by the statistical quantity $P$, which is calculated according to the following formula 7:

$$P = 2\,exp\left[-6k_{t_0}^2\left(n^3 + n^2\right)\right] \tag{7}$$

If $P$ is not larger than 0.5, then the detected abrupt change point is considered statistically significant.

### 2.3.3 Elasticity coefficient method
#### 2.3.3.1 Budyko Hypothesis

The Budyko theory (Budyko, 1974) is based on the water balance equation, which can be expressed as Equation 8:

$$R = P - ET + \Delta S \tag{8}$$

where, $R$ is the multi-year average streamflow depth, mm; $P$ is the multi-year average precipitation, mm; $ET$ is the multi-year average actual evapotranspiration, mm; and $\Delta S$ is the change in basin storage, mm.

After years of research, Budyko proposed that the multi-year evapotranspiration rate of a watershed is determined by PET and precipitation. Therefore, the Budyko Hypothesis can be simply expressed as Equation 9:

$$\frac{ET}{P} = f\left(\frac{ET_0}{P}\right) = f(\varphi) \tag{9}$$

where, $ET_0$ is the multi-year average PET, mm; $P$ is the multi-year average precipitation, mm, and $\varphi$ is the aridity index.

The original Budyko Hypothesis did not consider the effects of underlying surface conditions and watershed characteristics. Based on this, several studies have proposed a series of empirical Budyko formulas that incorporate parameters to represent underlying surface conditions (Milly and Dunne, 2002; Porporato et al., 2004). These formulas have been theoretically derived and validated. In this study, we selected the equations developed by Fu, Choudhury-Yang, and Zhang (Table 1) to attribute and identify the changes in watershed streamflow.

It is generally considered that the change in basin storage ($\Delta S$) can be neglected when studying closed watersheds over long-term hydrological sequences. In other words, under the assumption of

TABLE 1 Three Commonly Used Formulas based on the Budyko Hypothesis.

| Formula | Parameter | References |
|---|---|---|
| $ET/P = 1 + ET_0/P - [1 + (ET_0/P)^\omega]^{1/\omega}$ | $\omega$ | Fu et al. (2007), Wu et al. (2016) |
| $ET/P = 1/[1 + (P/ET_0)^n]^{1/n}$ | $n$ | Choudhury (1999), Yang et al. (2008) |
| $ET/P = [1 + \omega(ET_0/P)]/[1 + \omega(ET_0/P) + (ET_0/P)^{-1}]$ | $\omega$ | Zhang et al. (2001) |

In the Fu formula, the parameter $\omega$ reflects the underlying surface conditions of the watershed, which is related to land use, vegetation, soil, etc. In the Choudhury-Yang formula, the parameter $n$ has the same meaning as in the Fu formula. In the Zhang formula, the parameter $\omega$ represents the vegetation's effective water coefficient, indicating the relative differences in the way plants utilize soil moisture for transpiration. In this study, we use the unified notation "n" to represent these parameters.

constant basin storage, the water balance equation can be expressed as Equations 10–12:

$$R = P - \left( P + ET_0 - P\left(1 + \left(\frac{ET_0}{P}\right)^{n_{Fu}}\right)^{\frac{1}{n_{Fu}}}\right) \quad (10)$$

$$R = P - \frac{P \times ET_0}{\left(P^{n_{CY}} + ET_0^{n_{CY}}\right)^{\frac{1}{n_{CY}}}} \quad (11)$$

$$R = P - \frac{P + n_{Zh}ET_0}{1 + n_{Zh}\frac{ET_0}{P} + \left(\frac{ET_0}{P}\right)^{-1}} \quad (12)$$

### 2.3.3.2 Elasticity coefficients

Assuming that $P$, $ET_0$ and $n$ are independent variables and combining them with the water balance equation, the annual streamflow volume can be expressed in the form of a total differential, given by Equation 13:

$$dR = \frac{\partial R}{\partial P}dP + \frac{\partial R}{\partial ET_0}dET_0 + \frac{\partial R}{\partial n}dn \quad (13)$$

The sensitivity of streamflow volume $R$ to each influencing factor can be represented by the elasticity coefficient $\varepsilon$. The elasticity coefficient is defined as the degree of change in watershed streamflow resulting from a unit change in a climatic factor. It can be expressed as Equation 14:

$$\varepsilon_x = \frac{\partial R/R}{\partial x_i/x_i} \quad (14)$$

where, $\varepsilon_x$ is the sensitivity of streamflow volume to the influencing factor $x$, where $x$ can be $P$, $ET_0$, or $n$. Both $P$ and $ET_0$ are multi-year average values of the watershed.

### 2.3.3.3 Contribution of climate and underlying surface to streamflow variation

To quantitatively differentiate the contributions of various factors to streamflow variation, a complementary method based on the Budyko Hypothesis is employed. Zhou et al. proposed a complementary equation to separate the contributions of climate change and underlying surface change to streamflow variation, based on the complementary relationship of elasticity coefficients and the assumption of independence between $P$ and $ET_0$ (Zhou et al., 2015). This method eliminates theoretical calculation errors. The complementary relationship equation can be expressed as Equation 15:

$$\frac{\partial R/R}{\partial P/P} + \frac{\partial R/R}{\partial ET_0/ET_0} = 1 \quad (15)$$

Due to the uncertainty associated with climate and underlying surface conditions, the complementary relationship weighted factor method based on the Budyko Hypothesis introduces the weighting factors α to represent different pathways of change (Zhou et al., 2016). Through algebraic identity derivation, the complementary method for attributing streamflow variation is proposed. The expression can be given as Equation 16:

$$\Delta R = \alpha\left[\left(\frac{\partial R}{\partial P}\right)_1 \Delta P + \left(\frac{\partial R}{\partial ET_0}\right)_1 \Delta ET_0 + P_2\Delta\left(\frac{\partial R}{\partial P}\right) + E_{0,2}\Delta\left(\frac{\partial R}{\partial ET_0}\right)\right]$$

$$+ (1-\alpha)\left[\left(\frac{\partial R}{\partial P}\right)_2 \Delta P + \left(\frac{\partial R}{\partial ET_0}\right)_2 \Delta ET_0 + P_1\Delta\left(\frac{\partial R}{\partial P}\right) + E_{0,1}\Delta\left(\frac{\partial R}{\partial ET_0}\right)\right] \quad (16)$$

where, $\Delta R$ is the change in streamflow volume, mm; α is the weighting factor ($0 \leq \alpha \leq 1$), which is the contribution of different pathways of climate change and human activities to the changes in streamflow volume. In this study, $\alpha$ is set to 0.5. Subscripts 1 and 2 are the baseline period and abrupt change period before and after the abrupt change point, respectively. The formulas for calculating the changes in precipitation, evapotranspiration, and underlying surface, denoted as $\Delta R_P$, $R_{ET_0}$ and $\Delta R_n$ are as Equations 17–19:

$$\Delta R_P = \alpha\left[\left(\frac{\partial R}{\partial P}\right)_1 \Delta P\right] + (1-\alpha)\left[\left(\frac{\partial R}{\partial P}\right)_2 \Delta P\right] \quad (17)$$

$$\Delta R_{ET_0} = \alpha\left[\left(\frac{\partial R}{\partial ET_0}\right)_1 \Delta ET_0\right] + (1-\alpha)\left[\left(\frac{\partial R}{\partial ET_0}\right)_2 \Delta ET_0\right] \quad (18)$$

$$\Delta R_n = \alpha\left[P_2\Delta\left(\frac{\partial R}{\partial P}\right) + E_{0,2}\Delta\left(\frac{\partial R}{\partial ET_0}\right)\right] + (1-\alpha)\left[P_1\Delta\left(\frac{\partial R}{\partial P}\right) + E_{0,1}\Delta\left(\frac{\partial R}{\partial ET_0}\right)\right] \quad (19)$$

### 2.3.4 Hydrological simulation method

The WATLAC hydrological model (Li et al., 2016; Li et al., 2021; Ren et al., 2017; Ye et al., 2011) is a distributed hydrological model that simulates the surface and subsurface streamflow processes in a watershed driven by rainfall and evaporation. It incorporates processes such as vegetation interception, soil water storage, surface streamflow, soil recharge to groundwater, and saturated groundwater movement. The model adopts spatial discretization based on grid cells to simulate surface streamflow and the flow paths are determined based on terrain elevation and the water network. Groundwater movement is simulated by MODFLOW with finite difference grid discretization in space and coupling with the surface streamflow model to facilitate data transfer within the program. The finite difference grid used for groundwater
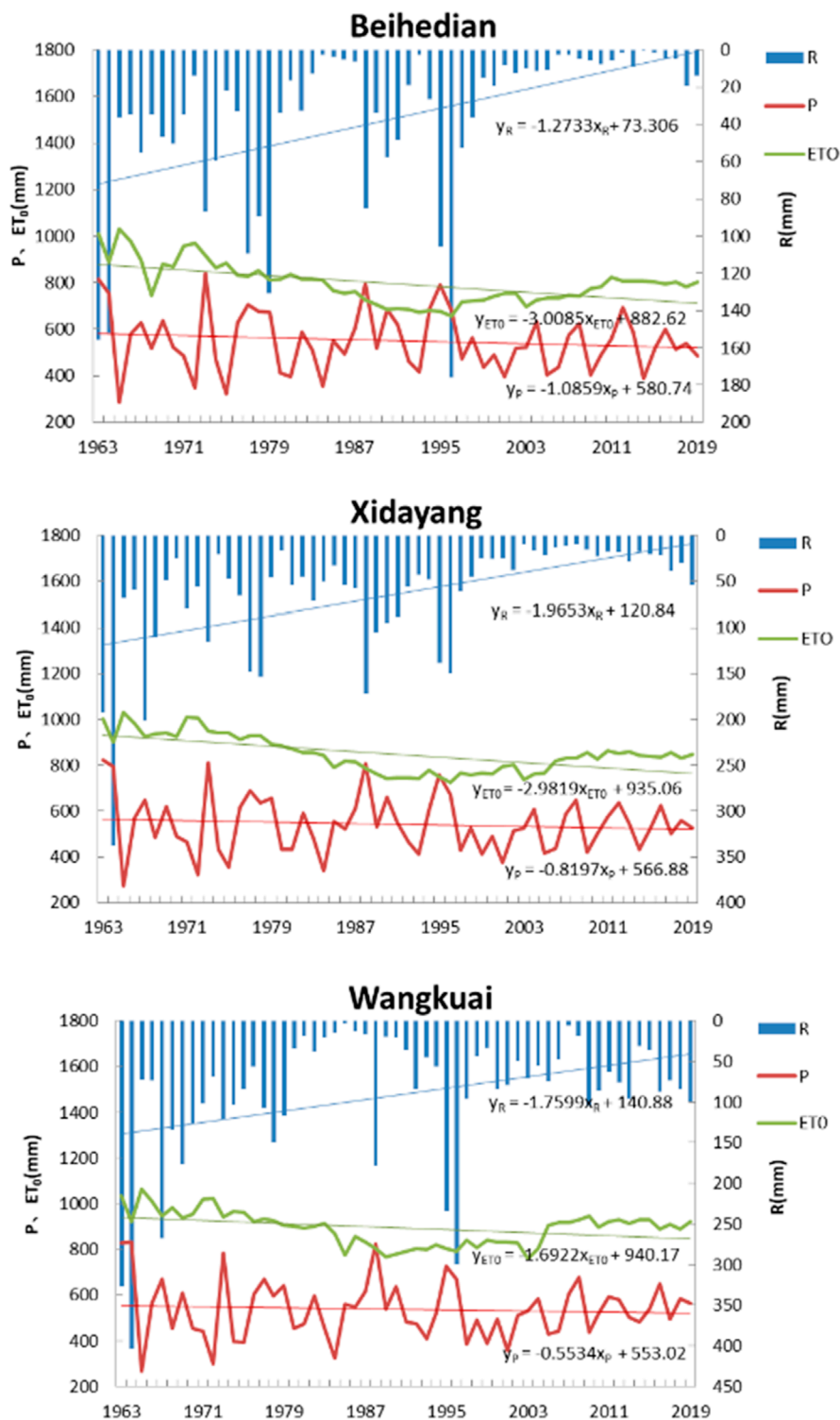
FIGURE 2
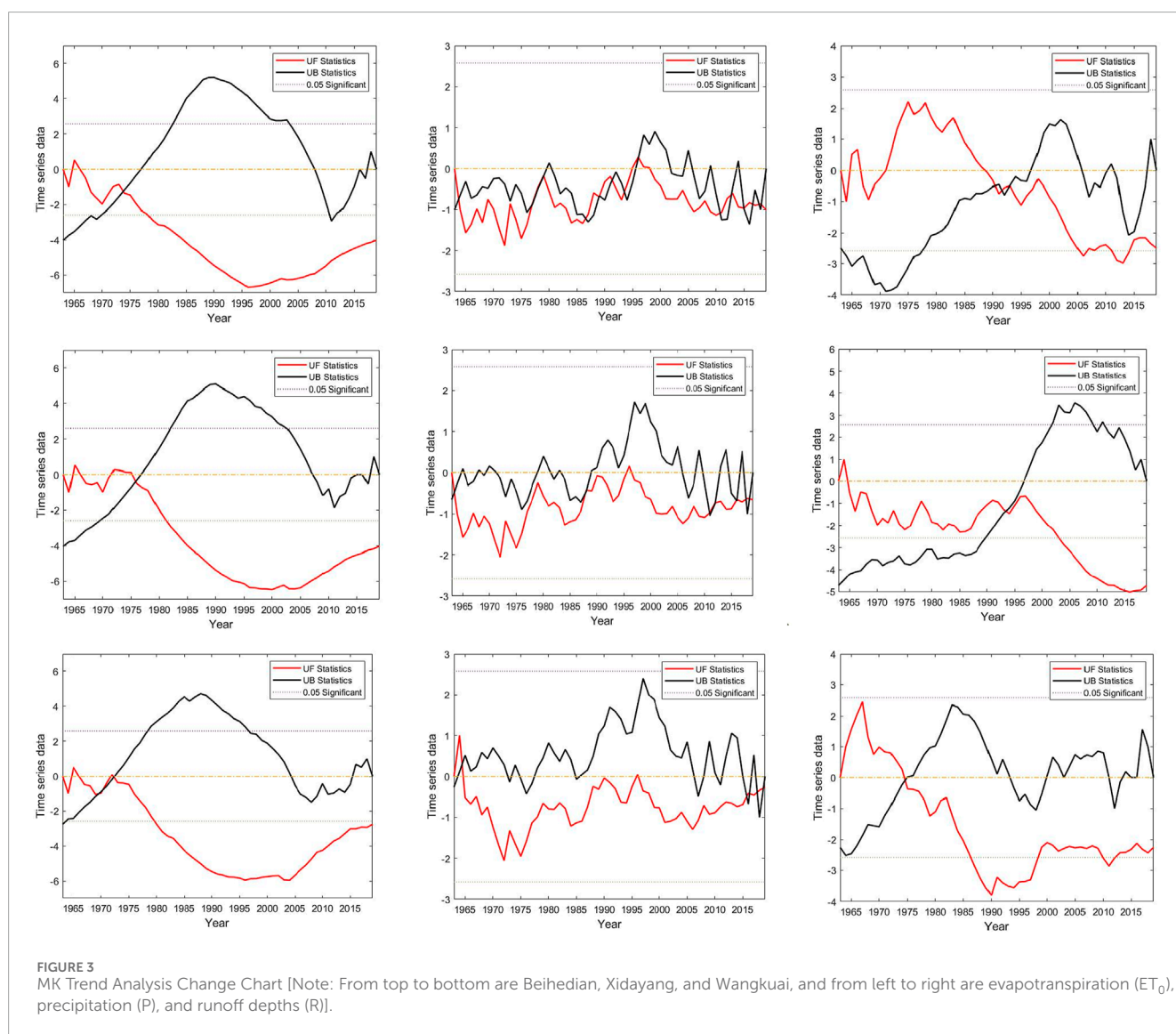Analysis results of linear estimation method.

simulation matches the planar grid cells used for surface water simulation on the horizontal plane. The WATLAC hydrological model allows for variable time steps for surface and subsurface streamflow, considering the differences in flow velocity between the two components and reducing the computational workload for groundwater simulation. Moreover, the model enables the quantitative differentiation of different streamflow components and provides detailed water balance outputs.

TABLE 2 MK trend analysis statistical results table.

| Small watershed | Meteorological stations | Area/km$^2$ | MK trend test Z-value | | | Coefficient of variation Cv | | |
|---|---|---|---|---|---|---|---|---|
| | | | R | P | ET$_0$ | R | P | ET$_0$ |
| Beihedian | Yixian, Laiyuan, Xiayunling | 6,854 | −4.91$^{**}$ | −0.99 | −3.91$^{**}$ | 1.21 | 0.96 | 0.96 |
| Xidayang | Lingqiu, Quyang | 4,413 | −4.61$^{**}$ | −0.64 | −3.94$^{**}$ | 1.03 | 0.95 | 0.96 |
| Wangkuai | Fuping, Wutaixian | 3,761 | −1.72$^{*}$ | −0.26 | −2.70$^{**}$ | 1.06 | 0.95 | 0.96 |

$^*$and$^{**}$indicate significance tests at the confidence levels of $p<0.05$ and $p<0.01$, respectively.



FIGURE 3
MK Trend Analysis Change Chart [Note: From top to bottom are Beihedian, Xidayang, and Wangkuai, and from left to right are evapotranspiration (ET$_0$), precipitation (P), and runoff depths (R)].

This paper employs the WATLAC hydrological model. Based on the change-point analysis of hydrometeorological data, the long-term data are divided into a baseline period and an abrupt change period. The meteorological data, soil data, and river data from the baseline period are used as inputs to simulate the watershed streamflow. The model parameters are calibrated by observed streamflow data. Using the well-calibrated model, the meteorological data from the abrupt change period are substituted for the original baseline period data to simulate the abrupt change period streamflow in the watershed. The quantitative relationship between the abrupt change in climate change and human activities is then analyzed.
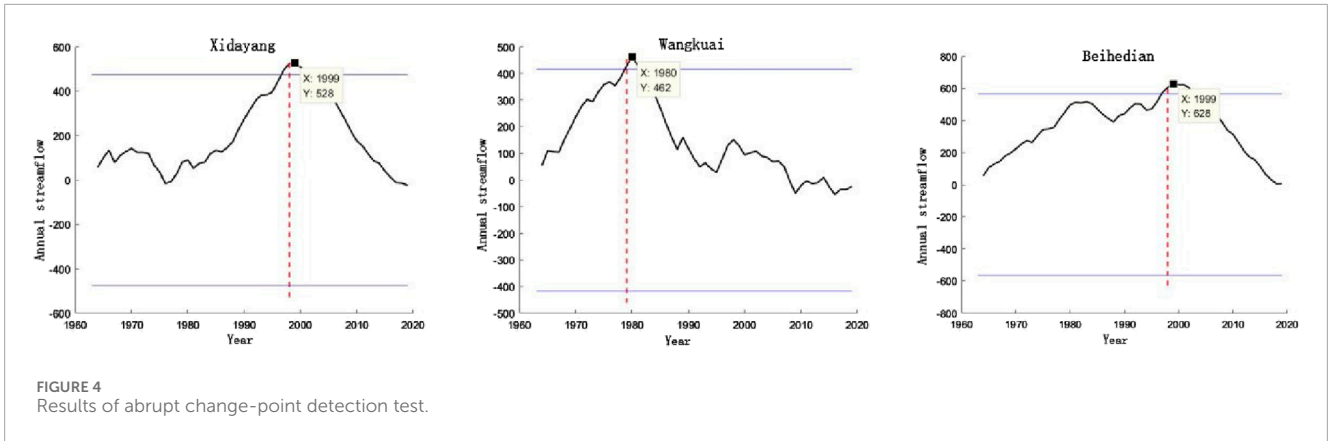
**FIGURE 4**
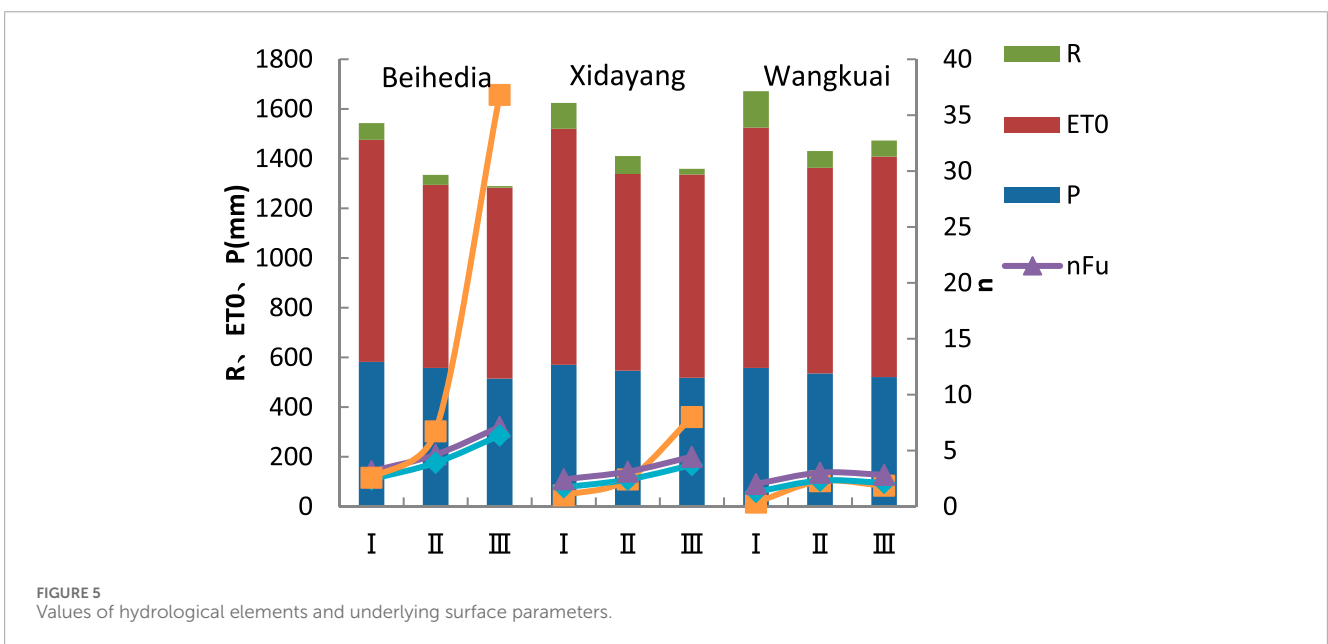Results of abrupt change-point detection test.



**FIGURE 5**
Values of hydrological elements and underlying surface parameters.

The Nash-Sutcliffe efficiency (NSE) is used as the objective function for parameter calibration. The calculation formula is as Equation 20:

$$NSE = 1 - \frac{\sum_{i=1}^{n}(Q_0 - Q_m)^2}{\sum_{i=1}^{n}(Q_0 - \overline{Q_0})^2} \qquad (20)$$

where $Q_0$ is the measured values; $Q_m$ is the simulated values; $\overline{Q_0}$ is the average value of the measured values; and n is the length of the streamflow series.

The NSE quantitatively indicates the goodness-of-fit of the entire modeling process and serves as a dimensionless statistical parameter to assess the accuracy of the simulated values compared to the measured values. An NSE value of 1 indicates a perfect match between the simulated values and the measured values. If NSE is negative, it indicates that the credibility of the model's simulated values is lower than that of directly using the measured average value.

# 3 Results

## 3.1 Trend Analysis Results

An overall decreasing trend in streamflow depth, precipitation, and PET for the three watersheds over the past 60 years can be obtained in Figure 2. The decreasing trends for the three variables are consistent across the different watersheds, indicating a high degree of similarity. The interannual variation range of streamflow depth varies between 3.97 and 404.33 mm, 9.20–338.07 mm, and 0–176.03 mm, indicating significant fluctuations and differences between wet and dry seasons (Figure 2). For example, in the control watershed of Xidayang Reservoir Station, the maximum streamflow depth occurred in 1964 with a value of 338.07 mm, while the minimum streamflow depth was recorded in 2008 with a value of 9.20 mm (Figure 2). The overall decrease rate of precipitation was the lowest, ranging from −1.09 to −0.55 mm/a. The decrease in precipitation was smaller than the decrease in streamflow depth, indicating that variables other than precipitation changes also affect streamflow reduction. On the other hand, the decrease in PET did

FIGURE 6
Result of sensitivity analysis.



FIGURE 7
Result of quantitative analysis.
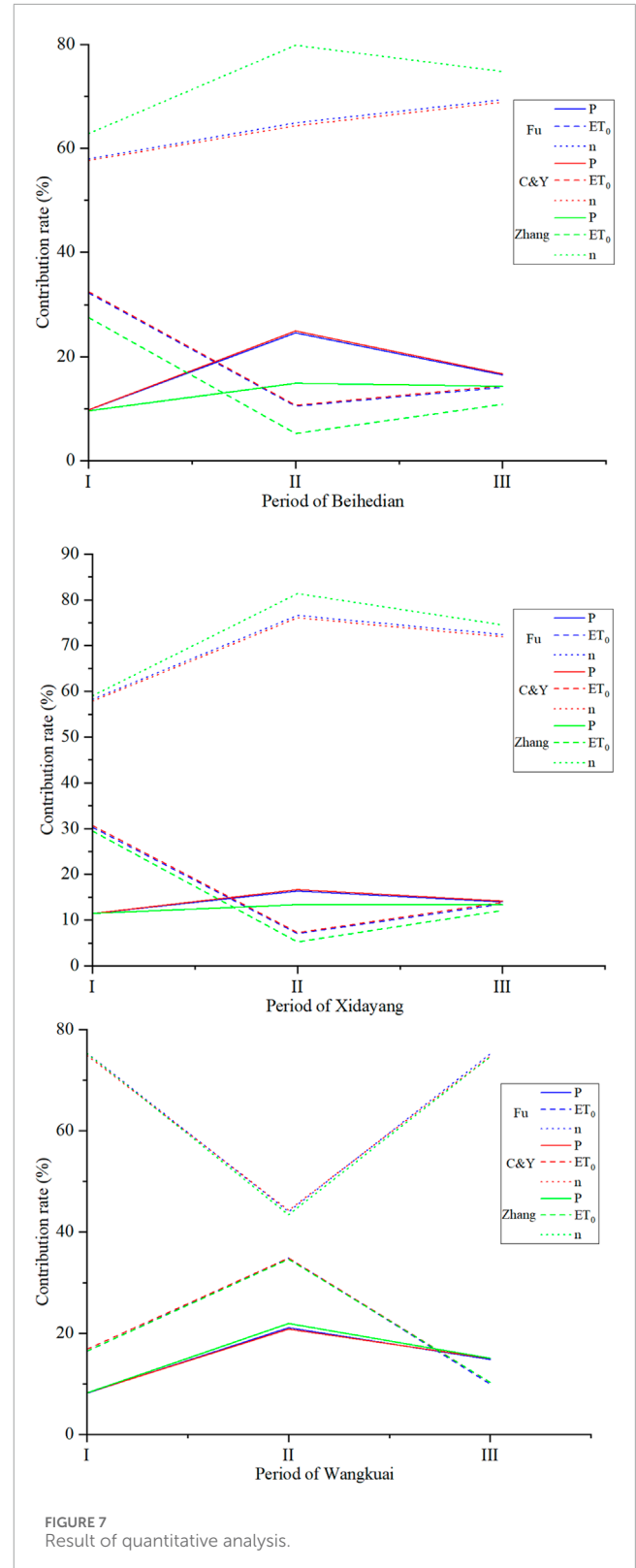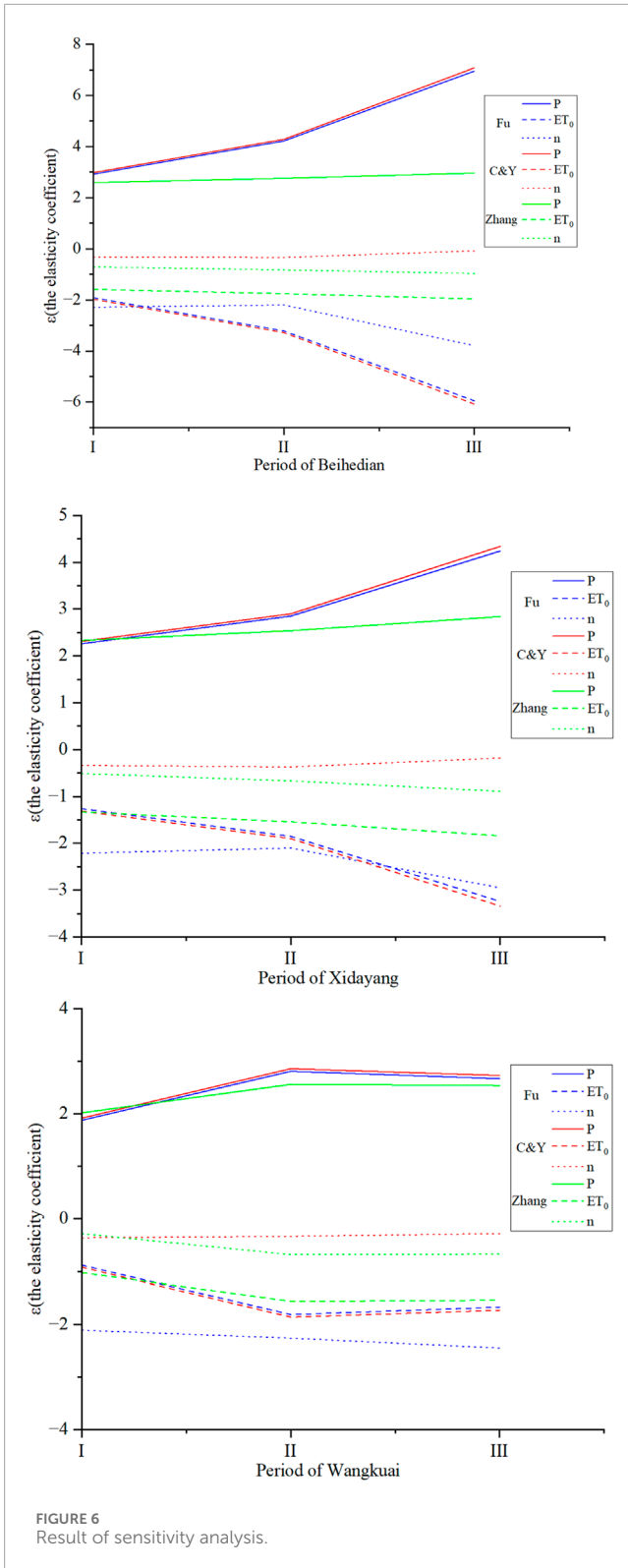
not lead to an increase in streamflow depth. This may be due to the moderate impact of a decrease in PET on streamflow when PET is greater than precipitation. The streamflow depth exhibited a decreasing trend in all three small watersheds, with decreasing rates of −1.76 mm/a, −1.97 mm/a, and −1.32 mm/a, respectively.

The Z-values obtained from the Mann-Kendall test for streamflow, precipitation, and PET in the three watersheds are all less than 0 (Table 2; Figure 3). This indicates that all variables exhibit a decreasing trend, which is consistent with the results

TABLE 3 Sensitivity of runoff to precipitation, PET, and underlying surface parameters.

| Small watershed | Time interval | Fu | | | Choudhury&Yang | | | Zhang | | |
|---|---|---|---|---|---|---|---|---|---|---|
| | | $\varepsilon_p$ | $\varepsilon_{ET0}$ | $\varepsilon_n$ | $\varepsilon_p$ | $\varepsilon_{ET0}$ | $\varepsilon_n$ | $\varepsilon_p$ | $\varepsilon_{ET0}$ | $\varepsilon_n$ |
| Beihedian | 1963–1979 | 2.92 | −1.92 | −2.29 | 2.98 | −1.98 | −0.32 | 2.59 | −1.59 | −0.71 |
| | 1980–1998 | 4.22 | −3.22 | −2.20 | 4.28 | −3.28 | −0.34 | 2.76 | −1.76 | −0.83 |
| | 1999–2019 | 6.95 | −5.95 | −3.79 | 7.08 | −6.08 | −0.08 | 2.96 | −1.96 | −0.97 |
| Xidayang | 1963–1979 | 2.26 | −1.26 | −2.21 | 2.31 | −1.31 | −0.34 | 2.33 | −1.33 | −0.51 |
| | 1980–1998 | 2.85 | −1.85 | −2.10 | 2.90 | −1.90 | −0.37 | 2.54 | −1.54 | −0.67 |
| | 1999–2019 | 4.24 | −3.24 | −2.95 | 4.34 | −3.34 | −0.18 | 2.84 | −1.84 | −0.89 |
| Wangkuai | 1963–1979 | 1.88 | −0.88 | −2.11 | 1.92 | −0.92 | −0.36 | 2.02 | −1.02 | −0.28 |
| | 1980–1998 | 2.81 | −1.81 | −2.26 | 2.86 | −1.86 | −0.33 | 2.56 | −1.56 | −0.68 |
| | 1999–2019 | 2.67 | −1.67 | −2.45 | 2.73 | −1.73 | −0.28 | 2.54 | −1.54 | −0.67 |

TABLE 4 Contribution rates of climate change and human activities to runoff.

| Study area | Base period | Mutation period | FU(%) | | | Choudhury&Yang (%) | | | Zhang (%) | | |
|---|---|---|---|---|---|---|---|---|---|---|---|
| | | | $\Delta R_P$ | $\Delta R_{ET_0}$ | $\Delta R_n$ | $\Delta R_P$ | $\Delta R_{ET_0}$ | $\Delta R_n$ | $\Delta R_P$ | $\Delta R_{ET_0}$ | $\Delta R_n$ |
| Beihedian | 1963–1979 | 1980–1998 | 9.75 | 32.27 | 57.98 | 9.77 | 32.53 | 57.70 | 9.59 | 27.55 | 62.86 |
| | 1980–1998 | 1999–2019 | 24.61 | 10.47 | 64.92 | 24.97 | 10.67 | 64.36 | 14.90 | 5.24 | 79.86 |
| | 1963–1979 | 1999–2019 | 16.51 | 14.12 | 69.38 | 16.70 | 14.40 | 68.90 | 14.33 | 10.85 | 74.81 |
| Xidayang | 1963–1979 | 1980–1998 | 11.43 | 30.31 | 58.26 | 11.43 | 30.68 | 57.88 | 11.49 | 29.47 | 59.03 |
| | 1980–1998 | 1999–2019 | 16.34 | 7.06 | 76.60 | 16.65 | 7.25 | 76.10 | 13.37 | 5.23 | 81.40 |
| | 1963–1979 | 1999–2019 | 13.99 | 13.55 | 72.46 | 14.17 | 13.89 | 71.95 | 13.34 | 12.12 | 74.54 |
| Wangkuai | 1963–1979 | 1980–1998 | 8.17 | 16.46 | 75.38 | 8.23 | 16.85 | 74.92 | 8.21 | 16.47 | 75.32 |
| | 1980–1998 | 1999–2019 | 21.09 | 34.87 | 44.04 | 20.83 | 34.87 | 44.30 | 21.93 | 34.66 | 43.41 |
| | 1963–1979 | 1999–2019 | 14.82 | 9.95 | 75.23 | 15.02 | 10.28 | 74.70 | 15.05 | 10.31 | 74.63 |

obtained from the linear propensity estimation method. At the same time, it further demonstrates that the results of linear propensity estimation are reasonable and reliable. Additionally, the PET in all three watersheds shows a significant decreasing trend and passes the significance test at a confidence level of 99% (Table 2). The decreasing trend in runoff depth in the Wangkuai River watershed is lower compared to the other two watersheds, only passing the significance test at a confidence level of $P < 0.05$ (Table 2). This indicates that the degree of runoff reduction in the Wangkuai Reservoir watershed during the study period was not as severe as the other two watersheds. However, the decreasing trend in annual precipitation is not significant and does not pass the significance test. Therefore, the annual precipitation in the three river basins did not

decrease continuously during the study period, but instead showed alternating periods of high and low rainfall (Figure 3). Furthermore, the Cv of runoff depth, precipitation, and evapotranspiration are similar among the three basins. This also shows the fluctuation levels of the variables in the three watersheds are similar, indicating a high level of consistency among the watersheds.

## 3.2 Change-point Analysis Results

The Pettitt abrupt change-point detection test was applied to detect the abrupt change points in the annual streamflow series of the Xidayang Reservoir Hydrological Station, Wangkuai Reservoir
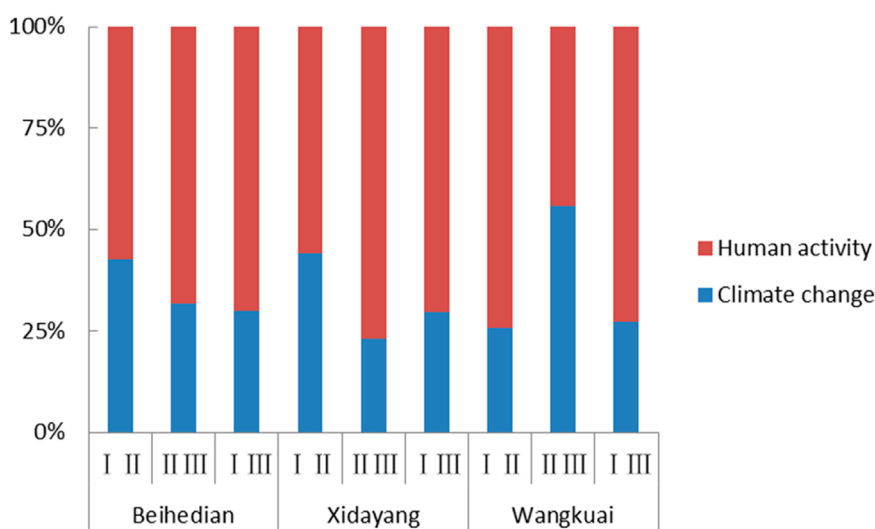
**FIGURE 8**
Proportion of climate change and human activities impact obtained by hydrological simulation method.
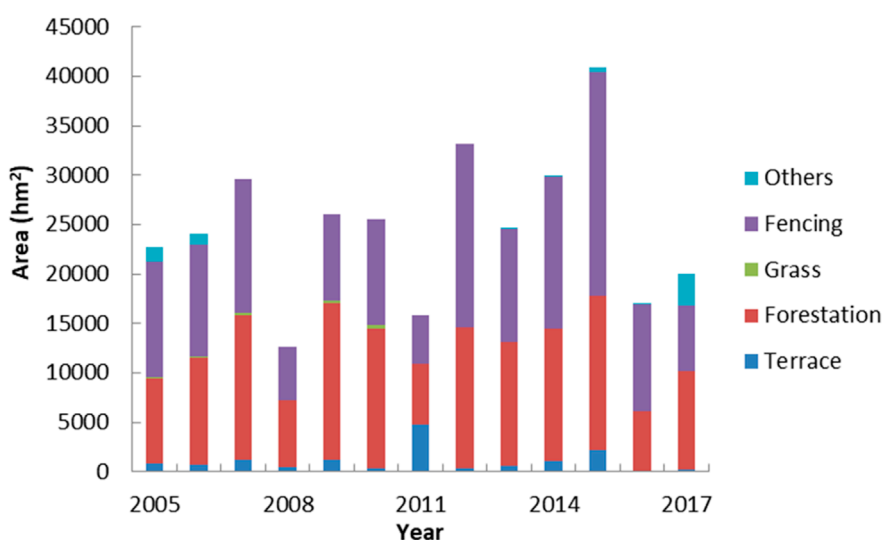


**FIGURE 9**
Completion status of various treatment measures.

Hydrological Station, and Beihedian Hydrological Station from 1963 to 2019. The Pettitt statistic for the Xidayang Reservoir Station and Beihedian Station fluctuated and increased before 1999 but decreased afterward, reaching a significant level of $\alpha=0.05$ (Figure 4). This indicates that both stations experienced a significant change point around 1999. On the other hand, the streamflow series of the Wangkuai Reservoir Station showed a significant change point around 1980 (Figure 4). This could be attributed to the implementation of land system reforms and the construction of the Three-North Shelterbelt Forest Program in China during the mid to late 1970s (Huang, 2018). These initiatives led to improved forest quality in the watershed, significantly increased vegetation coverage, and enhanced plant transpiration. Combined with the effects of

meteorological conditions such as precipitation and temperature, these factors contributed to the decrease in watershed streamflow. Therefore, the derived change points in the watershed streamflow are considered reasonable, and the results of the abrupt change-point detection test are consistent with those of relevant studies, confirming the reliability of the conclusions.

Based on the analysis of the change points in the three hydrological stations, the years 1980 and 1999 were selected as the change years. The period 1963–1979 (Period I) was designated as the natural baseline period. During this period, the hydrometeorological variables were relatively stable and there was minimal human interference that could impact streamflow. The period 1980–2019 represented the period of human activities'

**FIGURE 10**
Completion status of various treatment measures.
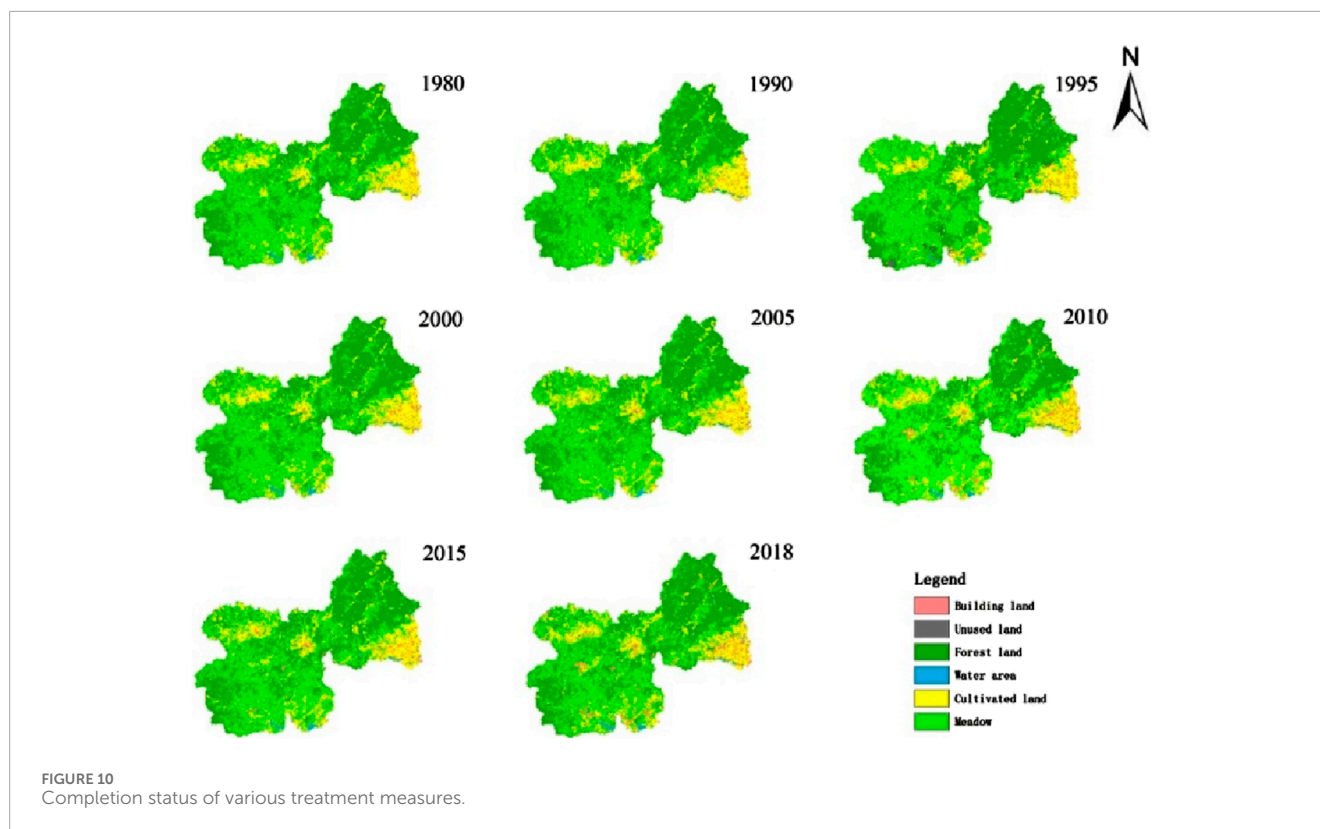
influence on streamflow and was further divided into two periods: 1980–1998 (Period II) and 1999–2019 (Period III). These periods experienced intense human activities such as water conservancy construction, afforestation, and increased water consumption, which resulted in significant disturbances to the streamflow.

In this study, an analysis was conducted based on these three periods, and the values of hydro-meteorological variables within each period are shown in Figure 5. The results demonstrate a high level of consistency among the three methods. The parameter n, representing the underlying surface, shows an increasing trend in all three watersheds. This trend is particularly pronounced in the Beihedian River watershed, where the change from Period II to Period III is most significant. This indicates that the impacts of human activities such as water conservancy projects and afforestation on streamflow have been progressively intensifying year by year.

## 3.3 Calculation results from the elasticity coefficient method

### 3.3.1 Sensitivity analysis

The sensitivity of streamflow depth to precipitation, PET, and underlying surface parameters is analyzed by three methods based on the Budyko Hypothesis. In this study, the elasticity coefficient $\varepsilon_x$ is employed to quantitatively characterize the sensitivity of streamflow depth to these variables.

It is evident that precipitation is positively correlated with streamflow, while PET and underlying surface parameters are negatively correlated with streamflow (Table 3, Figure 6). Taking the

calculation results based on Zhang Lu's empirical formula as an example, for the Beihedian River watershed, a 10% increase in baseline precipitation corresponds to a 25.9% increase in streamflow depth, while a 10% decrease in PET and underlying surface parameters corresponds to a 15.9% and 7.1% increase in streamflow depth, respectively. Furthermore, the sensitivity of streamflow depth to both precipitation and PET in the Beihedian River watershed increases over time. The precipitation sensitivity coefficient increases from 2.92 to 6.95 and the PET sensitivity coefficient increases from 1.92 to 5.95. Similar patterns were observed in the Xidayang Reservoir watershed, where the sensitivity of streamflow depth to precipitation and Pet also increases over time. The precipitation sensitivity coefficient increases from 2.62 to 4.24 and the PET sensitivity coefficient increases from 1.26 to 3.24. In contrast to the above two watersheds, the Wangkuai Reservoir watershed exhibits an initially significant enhancement and then a slight weakening in the sensitivity of streamflow depth to precipitation and PET over time.

Regarding the elasticity coefficients of streamflow depth to underlying surface parameters in the three watersheds, there are discrepancies among the calculation results obtained from the three methods (Table 3, Figure 6). Notably, the calculation results based on the Choudhury-Yang Formula exhibit an opposite trend compared to the other methods. However, the overall observation of a weak increasing tendency in sensitivity indicates the increasing influence of human activities on streamflow variations.

### 3.3.2 Quantitative analysis

Based on the results of the abrupt change-point detection test for streamflow depth in the three watersheds, the study period is divided into three periods: before 1980, after 1999, and between 1980 and

**FIGURE 11**
Proportion of land use types in different watersheds.
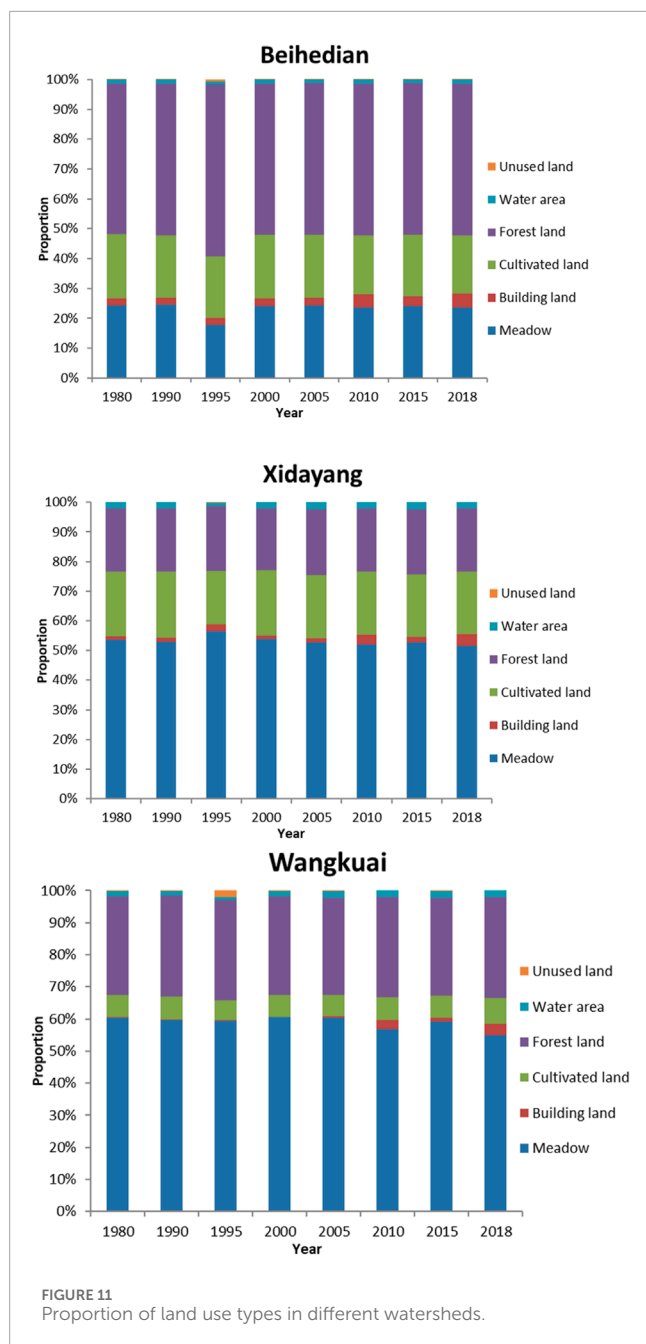
1999. Using formulas and three water balance equations based on the Budyko Hypothesis, the contribution rates of $P$, $ET_0$ and $n$ to the changes in streamflow depth are calculated.

Analysis of the data in Table 4, Figure 7 indicates that the results obtained from the three methods are relatively consistent, demonstrating a certain level of reliability. The impact of human activities on streamflow in the Beihedian River watershed is found to be above 57% and shows an increasing trend overall. In the Xidayang Reservoir watershed, the impact of human activities is higher compared to the other two watersheds, with the contribution rates in the order of Periods II and III, I and III, and I and II (Table 4, Figure 7). Moreover, the impact of human activities is more pronounced in Period III compared to Period II. Since the

year 2000, the intensification of human activities has led to a rapid decrease in streamflow. In contrast to the other two watersheds, the Wangkuai Reservoir watershed shows a lower contribution rate of human activities to streamflow, with the contribution rates in the order of Periods I and II, I and III, and II and III. The decreasing role of human activities in reducing streamflow has become weaker over time in this watershed.

## 3.4 Calculation results from the hydrological simulation method

In this study, the WATLAC hydrological model is employed to simulate three small watersheds within the study area at a spatial scale of 1 km and a daily time scale. Taking the Beihedian River watershed as an example for Periods I and II, the watershed data from Period I was used to build the model. The model was calibrated and parameterized using measured data, and the calibration results showed an NSE of 0.74 for this period, indicating a high accuracy and reliability of the model. To quantitatively assess the impacts of climate change and human activities on streamflow, the watershed data from Period II was used as input for the calibrated model to simulate the daily streamflow volume for that period. The difference between the simulated streamflow for Periods I and II was then calculated to represent the contribution of climate change to streamflow, and the contribution rate of human activities was determined accordingly.

Human activities have a significant influence in all three watersheds. Except for Periods II and III in the Wangkuai Reservoir watershed, human activities accounted for more than 50% of the influence on watershed streamflow in all three watersheds during the different periods. Particularly in the Xidayang Reservoir Basin during Periods II and III, human activities accounted for approximately 75% of the influence, far exceeding the 25% attributed to climate change's impact on watershed streamflow (Figure 8).

## 4 Discussion

### 4.1 Attribution analysis of precipitation runoff process

The formation and evolution of precipitation-streamflow processes are comprehensive processes influenced by a complex interplay between natural and human activities. These processes are affected by a multitude of factors. From the perspective of human activities, their impact on surface streamflow can be categorized into direct and indirect effects. The direct effects include activities such as water consumption, water induction projects, water diversion projects, and the construction of reservoirs (Shakarami et al., 2023).

The indirect effects primarily manifest in changes to the underlying surface of the watershed. Changes in land use types and alterations in vegetation cover can modify surface roughness (Bronstert et al., 2002; Zhang et al., 2007). These modifications can have profound effects on processes such as watershed streamflow yield, concentration, and evapotranspiration (Sterling et al., 2013; Xin et al., 2019). Such changes have significant implications for regional and even global water cycling processes and variations in water resources. Therefore, it is important to analyze

FIGURE 12
Changes in NDVI and precipitation in various watersheds.
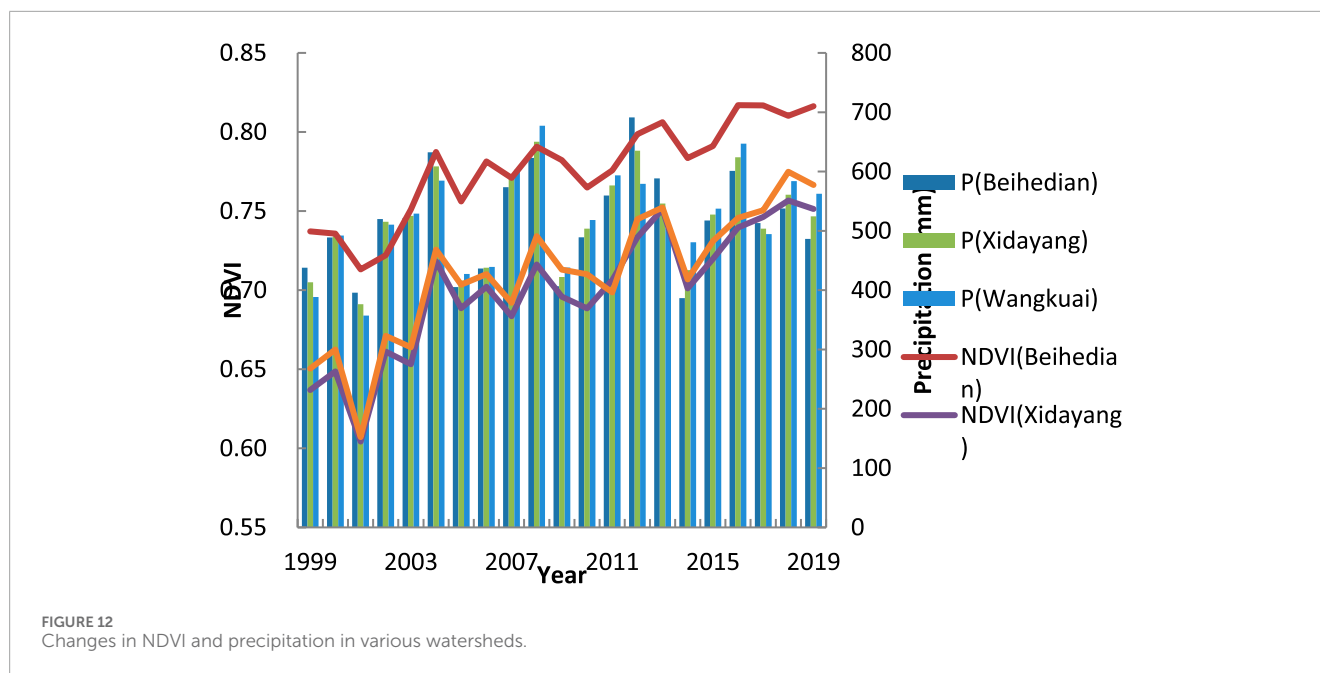
the four aspects of human activities that have a significant impact on human activities: soil erosion control, changes in land use types, changes in the fraction of vegetation cover (FVC), and changes in water consumption. This analysis will help clarify the causes of variations in streamflow.

Due to the combined effects of natural factors and human socioeconomic activities, severe soil erosion occurs in the mountainous area of the Daqing River Basin. It results in damage to water and soil resources as well as loss of land productivity. The watershed experiences frequent disasters such as heavy rainstorms, floods, dust storms, and sandstorms. For example, in 2005, the city of Baoding had a total area of soil erosion of 6,180 km$^2$, with moderate to severe erosion accounting for 72% of this area. Soil erosion is severe in the region. To improve the current ecological environment, various soil and water conservation measures were implemented in the city, including terracing, afforestation, grass planting, and the closure and management of degraded land. The status of these treatment measures can be seen in Figure 9. In 2020, the area affected by soil erosion in Baoding decreased to 4,345.96 km$^2$, with moderate to severe erosion covering 3.6% of this area. The area of soil erosion decreased by 1.27% compared to 2019 and by 29.68% compared to 2005, indicating significant effectiveness in soil and water conservation efforts (Figure 9). On one hand, soil and water conservation measures improve soil structure and result in increased soil porosity. This allows for greater infiltration depth and prolonged infiltration time, which in turn can intercept streamflow. On the other hand, these measures enhance the watershed's flood control and water storage capacity, thus affecting the collection of surface streamflow and increasing effective evaporation, thereby reducing the volume of river streamflow.

In order to visually demonstrate the impact of soil and water conservation measures on land use and vegetation cover in the watershed, an analysis of land use types from 1980 to 2019 was conducted for the typical years. Figures 10, 11 illustrate the spatial distribution changes of different land use types in the watershed

and their respective area proportions. It is evident that the main land use types in the study area are grassland, forestland, and farmland. Comparing Period III with Period II, there was a decrease in the area of farmland, grassland, and unused land, accompanied by an increase in forestland, which became the dominant land use type in the watershed. This change can be attributed to large-scale deforestation and cultivation on slopes that occurred from the late 1950s to the early 1960s, resulting in significant alternations to land use and damage to natural vegetation. Since the late 1970s, extensive soil and water conservation projects have been implemented in the watershed. In the early 1980s, largescale afforestation campaigns were carried out, leading to an increase in the forestland area within the watershed. The expansion of forestland played a significant role in water conservation by enhancing soil water retention capacity and reducing surface streamflow volume. In the rainy season, a portion of rainfall may be converted into underground streamflow. These measures had a positive effect on controlling flood and maintaining river flow during the dry season, increasing the low-flow volume and ensuring stable river discharge. However, it is important to note that the study area has deep soil layers and belongs to a semiarid region where vegetation transpiration consumes a significant amount of water. Therefore, the regulating effect of forest vegetation on river flow during the dry season is limited. In fact, during the dry season, vegetation can further intercept and retain streamflow by absorbing soil moisture through root growth. This can lead to drier soil conditions and increased storage of precipitation, further exacerbating the impact on streamflow.

Under the influence of human activities, changes occur in soil erosion, land use types, etc., thereby affecting the values of underlying surface parameters (Jiang et al., 2015). Among these parameters, the underlying surface parameter n is mainly influenced by factors such as vegetation, soil, and topography, while the variability of soil properties and topography within the watershed is relatively weak over a short period. Changes in the underlying surface parameters are mainly related to vegetation. Therefore, NDVI is selected as a

parameter to reflect vegetation growth status and analyze the impact of human activities and climate change on the underlying surface. It exhibits a linear relationship with chlorophyll density and vegetation productivity. And precipitation plays a very important role in the growth process of plants, so we simply consider precipitation as a factor in climate change. Figure 12 displays the changes in NDVI and precipitation. It can be observed that the overall NDVI values are relatively small with significant fluctuations but show an upward trend. Although both climate change and human activities can contribute to changes in underlying surface conditions, the increase in NDVI within the watershed is primarily influenced by human activities due to the insignificant changes in precipitation.

In the early 1980s, China implemented land reform policies, which encouraged farmers to increase agricultural activities to boost agricultural production. This resulted in a significant increase in grain output. However, water productivity remained relatively unchanged. As a consequence, there was an increase in agricultural water usage (Hu et al., 2012). Taking the city of Baoding as an example, the irrigated area was $6,573.33 \text{ km}^2$ in 2008, four times that of the early days of the People's Republic of China and twice that of 1957. Despite this expansion, large-scale flooding irrigation practices persist in the watershed, with a lack of water-saving measures. To meet irrigation needs, a large amount of groundwater is extracted, leading to the formation of extensive, deep underground cones of depression. This increases the extent of the unsaturated zone in the soil and its water storage capacity, thereby reducing streamflow formation. Furthermore, the significant decline in groundwater levels increases the hydraulic gradient between surface water and groundwater, leading to increased infiltration and further reducing the volume of surface streamflow.

The explosive growth of urban, industrial, mining, and residential land from 2000 to 2018 (Figure 11) indicates an accelerated pace of urbanization and rapid socioeconomic development. The proportion of industrial land is continuously rising, reflecting higher levels of urbanization. With the increase in population. and the demand for domestic and industrial water, the main water supply methods are through water diversion projects and groundwater extraction. However, engineering water induction directly reduces the flow in river channels, leading to a decline in surface streamflow. Moreover, the conversion of urban development land to impermeable hardened surfaces results in a rapid increase in surface streamflow and evaporation loss during heavy rainfall events, further reducing streamflow volume.

Based on the findings of this study, the following recommendations are proposed for the sustainable utilization and management of water resources in the watershed: In the field of agriculture, it is important to strengthen regulations on total water usage and efficiency, adjust planting structures, and actively promote water-saving technologies such as drip and sprinkler irrigation, while gradually advancing industrial upgrades. In the industrial sector, efforts should be closely aligned with industrial layout and urban planning, aiming to phase out high-water-consumption and heavily polluting enterprises, and to improve industrial water efficiency and recycling rates. In urban development, there should be a strong emphasis on promoting public water conservation initiatives, enhancing water quota management, and implementing water-saving measures for urban residents.

# 5 Conclusion

This study focuses on three small watersheds in the upstream mountainous areas of the Daqing River Basin. Attribution analysis of streamflow changes was conducted from the perspectives of climate change and human activities. The main factors influencing streamflow changes in the watershed were explored. The conclusions are as follows:

(1) From 1963 to 2019, a significant decreasing trend was observed in both the annual streamflow depth and PET across the Beihedian River, Xidayang Reservoir, and Wangkuai Reservoir watersheds. The magnitude of the decrease was similar among these watersheds, indicating a high level of consistency. However, the decreasing trend in annual precipitation was not significant and did not pass the significance test.

(2) The streamflow series in the Wangkuai Reservoir and Beihedian River watersheds exhibited significant change points in 1999, whereas the streamflow series in the Xidayang Reservoir watershed experienced a significant change point in 1980. These change points may be related to the implementation of land system reforms and the construction of the Three-North Shelterbelt Forest Program in the mid to late 1970s.

(3) Based on the elasticity coefficient method and hydrological simulation method, consistent results were obtained: the average contribution rates of climate change to streamflow reduction in the three small watersheds were 32.93%, 34.50%, and 35.12%, respectively, while the average contribution rates of human activities were 67.07%, 65.50%, and 64.88%, respectively. Climate change has led to a reduction in streamflow volume in the watershed to some extent, but the primary reason for water resource depletion in the watershed is still the excessive interference of human activities.

## Data availability statement

The raw data supporting the conclusions of this article will be made available by the authors, without undue reservation.

## Author contributions

ZL: Data curation, Formal Analysis, Validation, Visualization, Writing–original draft, Writing–review and editing. WC: Conceptualization, Data curation, Formal Analysis, Methodology, Writing–review and editing. LW: Conceptualization, Formal Analysis, Methodology, Writing–review and editing.

## Funding

## Conflict of interest

The authors declare that the research was conducted in the absence of any commercial or financial relationships that could be construed as a potential conflict of interest.

## Publisher's note

All claims expressed in this article are solely those of the authors and do not necessarily represent those of their affiliated organizations, or those of the publisher, the editors and the reviewers. Any product that may be evaluated in this article, or claim that may be made by its manufacturer, is not guaranteed or endorsed by the publisher.

## References

Bronstert, A., Niehoff, D., and Bürger, G. (2002). Effects of climate and land-use change on storm runoff generation: present knowledge and modelling capabilities. *Hydrol. Process.* 16, 509–529. doi:10.1002/hyp.326

Budyko, M. (1974). *Climate and life*. New York, NY: Academic Press.

Cheng, D. M., Liu, X. H., Zhao, S. N., Cui, B. S., Bai, J. H., and Li, Z. j. (2017). Influence of the natural colloids on the multiphase distributions of antibiotics in the surface water from the largest lake in North China. *Sci. Total Environ.* 578, 649–659. doi:10.1016/j.scitotenv.2016.11.012

Chien, H. C., Yeh, P. J. F., and Knouft, J. H. (2013). Modeling the potential impacts of climate change on streamflow in agricultural watersheds of the Midwestern United States. *J. Hydrol.* 491 (1), 73–88. doi:10.1016/j.jhydrol.2013.03.026

Choudhury, B. (1999). Evaluation of an empirical equation for annual evaporation using field observations and results from a biophysical model. *J. Hydrol.* 216 (1-2), 99–110. doi:10.1016/S0022-1694(98)00293-5

Dai, G. H., Liu, X. H., Liang, G., Han, X., Shi, L., Cheng, D. M., et al. (2011). Distribution of organochlorine pesticides (OCPs) and polychlorinated biphenyls (PCBs) in surface water and sediments from Baiyangdian Lake in North China. *J. Environ. Sci.* 23 (10), 1640–1649. doi:10.1016/S1001-0742(10)60633-X

Deng, Q. H., Zhang, X. M., Zhang, L. Z., Shao, X., and Gu, T. S. (2024). The impact mechanism of human activities on the evolution of coastal wetlands in the Liaohe River Delta. *Front. Ecol. Evol.* 12. doi:10.3389/fevo.2024.1423234

Du, Y., Bao, A. M., Zhang, T., and Ding, W. (2023). Quantifying the impacts of climate change and human activities on seasonal runoff in the Yongding River basin. *Ecol. Indic.* 154, 110839. doi:10.1016/j.ecolind.2023.110839

Fu, G. B., Charles, S. P., and Chiew, F. H. S. (2007). A two-parameter climate elasticity of streamflow index to assess climate change effects on annual streamflow. *Water Resour. Res.* 43 (11), 2578–2584. doi:10.1029/2007WR005890

Hu, S. S., Liu, C. M., Zheng, H. X., Wang, Z. G., and Yu, J. J. (2012). Assessing the impacts of climate variability and human activities on streamflow in the water source area of Baiyangdian Lake. *J. Geog. Sci.* 22 (5), 895–905. doi:10.1007/s11442-012-0971-9

Huang, B. B. (2018). Drive factors of surface runoff changes between 1980-2010 in the mountainous areas of Haihe Basin. Master thesis *Adv. Meteorology*.

Huang, P., Song, J. X., Cheng, D. D., Sun, H. T., Kong, F. H., Jing, K. X., et al. (2021). Understanding the intraannual variability of streamflow by incorporating terrestrial water storage from GRACE into the Budyko framework in the Qinba Mountains. *J. Hydrol.* 603, 126988. doi:10.1016/j.jhydrol.2021.126988

Jiang, C., Xiong, L. H., Wang, D. B., Liu, P., Guo, S. L., and Xu, C. Y. (2015). Separating the impacts of climate change and human activities on runoff using the Budyko type equations with time-varying parameters. *J. Hydrol.* 522, 326–338. doi:10.1016/j.jhydrol.2014.12.060

Lei, H., Yang, D., and Huang, M. (2014). Impacts of climate change and vegetation dynamics on runoff in the mountainous region of the Haihe River basin in the past five decades. *J. Hydrol.* 511, 786–799. doi:10.1016/j.jhydrol.2014.02.029

Li, J. Z., Li, Y. P., Zhang, T., and Feng, P. (2023). Research on the future climate change and runoff response in the mountainous area of Yongding watershed. *J. Hydrol.* 625, 130108. doi:10.1016/j.jhydrol.2023.130108

Li, Y. L., Tao, H., Yao, J., and Zhang, Q. (2016). Application of a distributed catchment model to investigate hydrological impacts of climate change within Poyang Lake catchment (China). *Hydrol. Res.* 47, 120–135. doi:10.2166/nh.2016.234

Li, Y. L., Zhang, Q., Tao, H., and Yao, J. (2021). Integrated model projections of climate change impacts on water-level dynamics in the large Poyang Lake (China). *Hydrol. Res.* 52 (1), 43–60. doi:10.2166/nh.2019.064

Liang, W., Bai, D., Jin, Z., You, Y., Li, J., and Yang, Y. (2015). A study on the streamflow change and its relationship with climate change and ecological restoration measures in a sediment concentrated region in the loess plateau, China. *China. Water Resour. manage.* 29 (11), 4045–4060. doi:10.1007/s11269-015-1044-5

Liu, Q., Yang, D., and Cao, L. (2022). Evolution and prediction of the coupling coordination degree of production–living–ecological space based on land use dynamics in the Daqing River Basin, China. *Sustainability* 14, 10864. doi:10.3390/su141710864

Liu, T., Huang, H. Q., Shao, M. A., Cheng, J., Li, X. D., and Lu, J. H. (2020). Integrated assessment of climate and human contributions to variations in streamflow in the ten great gullies basin of the upper yellow river, China. *J. Hydrol. Hydromech.* 68, 249–259. doi:10.2478/johh-2020-0027

Lyu, X. L., Jia, Y. W., Qiu, Y. Q., Du, J. K., Hao, C. F., Dong, H., et al. (2024). Influence of human-induced land use change on hydrological processes in semi-humid and semi-arid region: a case in the Fenhe River Basin. *J. Hydrol-Reg Stud.* 51, 101605. doi:10.1016/j.ejrh.2023.101605

Milly, P. C. D., and Dunne, K. A. (2002). Macroscale water fluxes 2. Water and energy supply control of their interannual variability. *Water Resour. Res.* 38 (10), 24. doi:10.1029/2001WR000760

Moiwo, J. P., Yang, Y. H., Li, H. L., Han, S. M., and Yang, Y. M. (2010). Impact of water resource exploitation on the hydrology and water storage in Baiyangdian Lake. *Hydrol. Process* 24 (21), 3026–3039. doi:10.1002/hyp.7716

Porporato, A., Daly, E., and Rodriguez-Iturbe, I. (2004). Soil water balance and ecosystem response to climate change. *Am. Nat.* 164 (5), 625–632. doi:10.1086/424970

Qiao, Z. X., Ma, L., Xu, Y., Yang, D. W., Liu, T. X., and Sun, B. L. (2023). Runoff change and attribution analysis in a semiarid mountainous basin. *Ecol. Eng.* 195, 107075. doi:10.1016/j.ecoleng.2023.107075

Ren, L., Xiang, X. Y., and Liu, W. L. (2017). River runoff changes in the past millennium under extreme climatic conditions in China. *Appl. Ecol. Env. Res.* 15 (4), 1157–1166. doi:10.15666/aeer/1504_11571166

Shakarami, L., Ashofteh, P. S., and Singh, V. P. (2023). Disaggregating the effects of climatic variability and dam construction on river flow regime. *Water Resour. Manag.* 36 (10), 3813–3838. doi:10.1007/s11269-022-03235-9

Song, C. Q., Ke, L. H., Pan, H., Zhan, S. G., Liu, K., and Ma, R. H. (2018). Long-term surface water changes and driving cause in Xiong'an, China:from dense Landsat time series images and synthetic analysis. *Sci. Bull.* 63 (11), 708–716. doi:10.1016/j.scib.2018.05.002

Sterling, S. M., Ducharne, A., and Polcher, J. (2013). The impact of global land-cover change on the terrestrial water cycle. *Nat. Clim. Chang.* 3, 385–390. doi:10.1038/NCLIMATE1690

Wang, D. D., Yu, X. X., Jia, G. D., and Wang, H. N. (2019). Sensitivity analysis of runoff to climate variability and landuse changes in the Haihe Basin mountainous area of north China. *Agr Ecosyst. Environ.* 269, 193–203. doi:10.1016/j.agee.2018.09.025

Wang, H. N., Lv, X. Z., and Zhang, M. Y. (2021). Sensitivity and attribution analysis based on the Budyko hypothesis for streamflow change in the Baiyangdian catchment, China. *Ecol. Indic.* 121, 107221. doi:10.1016/j.ecolind.2020.107221

Wu, J. K., Li, H. Y., Zhou, J. X., Tai, S. Y., and Wang, X. L. (2021). Variation of runoff and runoff components of the upper shule river in the northeastern qinghai–tibet plateau under climate change. *Water* 13, 3357. doi:10.3390/w13233357

Wu, J. W., Miao, C. Y., Wang, Y. M., Duan, Q., and Zhang, X. (2016). Contribution analysis of the long-term changes in seasonal runoff on the Loess Plateau, China, using eight Budyko-based methods. *J. Hydrol.* 545, 263–275. doi:10.1016/j.jhydrol.2016.12.050

Xin, Z. H., Li, Y., Zhang, L., Ding, W., Ye, L., Wu, J., et al. (2019). Quantifying the relative contribution of climate and human impacts on seasonal streamflow. *J. Hydrol.* 574, 936–945. doi:10.1016/j.jhydrol.2019.04.095

Xu, F., Yang, Z. F., Chen, B., and Zhao, Y. W. (2013). Impact of submerged plants on ecosystem health of the plant-dominated Baiyangdian Lake, China. *Ecol. Modell.* 252, 167–175. doi:10.1016/j.ecolmodel.2012.07.013

Yang, H., and Cao, J. (2021). Analysis of basin morphologic characteristics and their influence on the water yield of mountain watersheds upstream of the xiongan new area, north China. *North China. Water* 13, 2903. doi:10.3390/w13202903

Yang, H. B., Yang, D. W., Lei, Z. D., and Sun, F. (2008). New analytical derivation of the mean annual water-energy balance equation. *Water Resour. Res.* 44 (3), W03410. doi:10.1029/2007WR006135

Yang, J., Chang, J. X., Yao, J., Wang, Y. M., Huang, Q., and Xu, G. X. (2019). Impact of natural climate variability on runoff based on Monte Carlo method. *Water Clim. Change.* 10, 344–359. doi:10.2166/wcc.2017.177

Ye, X. C., Zhang, Q., Bai, L., and Hu, Q. (2011). A modeling study of catchment discharge to Poyang Lake under future climate in China. *Quat. Int.* 244 (2), 221–229. doi:10.1016/j.quaint.2010.07.004

Zeng, F., Ma, M. G., Di, D. R., and Shi, W. Y. (2020). Separating the impacts of climate change and human activities on runoff: a review of method and application. *Water* 12, 2201. doi:10.3390/w12082201

Zerizghi, T., Yang, Y., Wang, W., Zhou, Y., Zhang, J., and Yi, Y. (2020). Ecological risk assessment of heavy metal concentrations in sediment and fish of a shallow lake: a case study of Baiyangdian Lake, North China Environ. *Monit. Assess.* 192, 1–16. doi:10.1007/s10661-020-8078-8

Zhang, J., and Yu, X. L. (2021). Analysis of land use change and its influence on runoff in the Puhe River Basin. *Environ. Sci. Pollut. R.* 28, 40116–40125. doi:10.1007/s11356-020-09798-7

Zhang, L., Dawes, W. R., and Walker, G. R. (2001). Response of mean annual evapotranspiration to vegetation changes at catchment scale. *Water Resour. Res.* 37 (3), 701–708. doi:10.1029/2000WR900325

Zhang, Q., Miao, C. Y., Guo, X. Y., Gou, J. J., and Su, T. (2023). Human activities impact the propagation from meteorological to hydrological drought in the Yellow River Basin, China. *J. Hydrol.* 623, 129752. doi:10.1016/j.jhydrol.2023.129752

Zhang, Q. F., Liu, J. K., Yu, X. X., and Chen, L. H. (2019). Scale effects on runoff and a decomposition analysis of the main driving factors in Haihe Basin mountainous area. *Sci. Total Environ.* 690, 1089–1099. doi:10.1016/j.scitotenv.2019.06.540

Zhang, X., Zwiers, F. W., Hegerl, G. C., Lambert, F. H., Gillett, N. P., Solomon, S., et al. (2007). Detection of human influence on twentieth-century precipitation trends. *Nature* 448, 461–465. doi:10.1038/nature06025

Zheng, D. D., Gui, Y. H., Kuang, J., and Bing, H. (2023). Downstream Channel evolution and its causes in the yuan river during the qing dynasty. *J. Earth Sci.* 34 (4), 1263–1271. doi:10.1007/s12583-021-1600-2

Zhou, S., Yu, B. F., Huang, Y. F., and Wang, G. (2015). The complementary relationship and generation of the Budyko functions. *Geophys. Res. Lett.* 42, 1781–1790. doi:10.1002/2015GL063511

Zhou, S., Yu, B. F., Zhang, L., Huang, Y., Pan, M., and Wang, G. (2016). A new method to partition climate and catchment effect on the mean annual runoff based on the Budyko complementary relationship. *Water Resour. Res.* 52 (9), 7163–7177. doi:10.1002/2016WR019046